Bacterial cellulose-lignin composite hydrogel as a promising agent in chronic wound healing

Danica Zmejkoski, Dragica Spasojević, Irina Orlovska, Natalia Kozyrovska, Marina Soković, Jasmina Glamočlija, Svetlana Dmitrović, Branko Matović, Nikola Tasić, Vuk Maksimović, Mikhail Sosnin, Ksenija Radotić

PII: S0141-8130(18)32091-9
DOI: doi:10.1016/j.ijbiomac.2018.06.067
Reference: BIOMAC 9907

To appear in: *International Journal of Biological Macromolecules*

Received date: 3 May 2018
Accepted date: 12 June 2018

Please cite this article as: Danica Zmejkoski, Dragica Spasojević, Irina Orlovska, Natalia Kozyrovska, Marina Soković, Jasmina Glamočlija, Svetlana Dmitrović, Branko Matović, Nikola Tasić, Vuk Maksimović, Mikhail Sosnin, Ksenija Radotić , Bacterial cellulose-lignin composite hydrogel as a promising agent in chronic wound healing. Biomac (2017), doi:10.1016/j.ijbiomac.2018.06.067

Bacterial cellulose-lignin composite hydrogel as a promising agent in chronic wound healing

Danica Zmejkoski[a], Dragica Spasojević[b], Irina Orlovska[c], Natalia Kozyrovska[c], Marina Soković[d], Jasmina Glamočlija[d], Svetlana Dmitrović[a], Branko Matović[a], Nikola Tasić[b], Vuk Maksimović[b], Mikhail Sosnin[e], Ksenija Radotić[b]

[a]Vinča Institute of Nuclear Sciences, University of Belgrade, Mihaila Petrovića Alasa 12-14, 11001 Belgrade, Serbia; danica@vinca.rs, svetlanadmitrovic1612@gmail.com, mato@vinca.rs

[b]Institute for Multidisciplinary Research, University of Belgrade, Kneza Višeslava 1, 11000 Belgrade, Serbia; dragica@imsi.rs, xenia@imsi.rs, maxivuk@imsi.rs, nikola.tasic@imsi.bg.ac.rs

[c]Institute of Molecular Biology and Genetics, National Academy of Sciences of Ukraine, Zabolotnogo Str. 150, Kyiv, Ukraine; i.vviki@ukr.net, kozyrna@ukr.net

[d]Institute for Biological Research 'Siniša Stanković', Mycological Laboratory, Department of Plant Physiology, University of Belgrade, Bulevar despota Stefana 142, 11000 Belgrade, Serbia; jasna@ibiss.bg.ac.rs, mris@ibiss.bg.ac.rs

[e]Institute of Physics, National Academy of Sciences of Ukraine, 46 Nauki Ave., 03028, Kyiv, Ukraine; lukh@iop.kiev.ua

Corresponding Author

Danica Zmejkoski, Vinča Institute of Nuclear Sciences, University of Belgrade, Mihaila Petrovića Alasa 12-14, 11001 Belgrade, Serbia; Phone: +381 11 6447 335; Fax: +381 11 3408 224; danica@vinca.rs, danica167@yahoo.com

Abstract

Lignins and lignin-derived compounds are known to have antibacterial properties. The wound healing agents in the form of dressings produce faster skin repair and decrease pain in patients. In order to create an efficient antimicrobial agent in the form of dressing in the treatment of chronic wounds, a composite hydrogel of bacterial cellulose (BC) and dehydrogenative polymer of coniferyl alcohol (DHP), BC-DHP, was designed. Novel composite showed inhibitory or bactericidal effects against selected pathogenic bacteria, including clinically isolated ones. The highest release rate of DHP was in the first hour, while after 24 h there was still slow release of small amounts of DHP from BC-DHP during 72 h monitoring. High-performance liquid chromatography coupled with mass-spectrometry showed that BC-DHP releases DHP oligomers, which are proposed to be antimicrobially active DHP fractions. Scanning electron microscopy and atomic force microscopy micrographs proved a dose-dependent interaction of DHP with BC, which resulted in a decrease of the pore number and size in the cellulose membrane. The Fourier-transform infrared absorption spectra of the BC-DHP showed that DHP was partly bound to the BC matrix. The swelling and crystallinity degree were dose-dependent. All obtained results confirmed BC-DHP composite as a promising hydrogel for wounds healing.

Keywords

lignin model polymer; bacterial cellulose; antimicrobial activity.

1. Introduction

Bacterial cellulose (BC) is a natural polymer synthesized by different acetic acid- and other bacteria, accomplished by the presence of carbon (fructose, glucose, sucrose, and xylose) and nitrogen sources in fermentation medium [1]. BC polymer as hydrogel displays high water content (up to 99%), good sorption of liquids, high wet strength, high chemical purity and can be safely sterilized without any change of its structure and properties [2]. BC as biocompatible material [3-5] increase interest in developing of wide range biomedical applications [6-8] and one of them is wound healing [9-11]. In this complex process, the moisture in wound provided by different dressings produces faster skin repair and decreases pain in patients. Capability to absorb exudate, but also to inhibit or stop the growth of microorganisms present in that kind of environment are an important characteristics of a good wound healing agent. It was already shown that BC provides rapid tissue regeneration and significant capillary formation in the wound area [12, 13], but without antibacterial effect. Novel composites assume adding the antimicrobial agents in BC to provide better wound healing agents. Some of those different agents are: benzalkonium chloride [14] copper, silver and ZnO nanoparticles [15-18], silver sulfadiazine [19], polyhexamethylene guanidine hydrochloride [20] etc. Recent studies reported composites of BC with organic natural materials, such as silk sericin [21, 22], chitosan [23] and propolis [24, 25] with antibacterial activity in wound healing.

BC porous structure allows high accessibility of compounds in the 3D network. The hydroxyl groups on the surface of BC provide the possibility of interaction by chemical bonds and electrostatic adsorption [26, 27]. In spite of growing number of publications about BC modifications for wound healing, there is a limiting application of BC composites as drug-delivery systems [28].

Lignin as the second most abundant biopolymer and lignin-derived compounds have been proposed to be a very good candidate in medicine and health maintenance as antimicrobials [29-32]. They are attractive candidate in hydrogels as multipurpose materials for extensive applications in different fields [33, 34]. In our recent work, we have shown that dehydrogenative polymer of coniferyl alcohol (DHP), enzymatically synthesized lignin model compound from coniferyl alcohol (CA), in a hydrogel with alginate showed a strong antibacterial activity, peculiarly against *Pseudomonas aeruginosa*, *Listeria monocytogenes*, *Staphylococcus aureus* and *Salmonella typhimurium* [35]. *P. aeruginosa* is the most common multi-drug resistant pathogen present in chronic wounds that may account for 10% of all hospital-acquired infections, and is also found in burns, post-surgical wounds, pressure injuries and diabetic foot wounds. Secretions of this microorganism form a biofilm, which protects the bacteria from antibiotics and the immune system, making it challenging to eradicate these bacteria [36, 37]. Biofilm-forming bacteria are recognized as a major impediment to wound healing. The efficacy of traditional wound care against biofilm-infected wounds is low, and there is a need to improve the design of the formulations of long-term release systems.

In this study we report the characterization of the BC-DHP hydrogel as the formulation of long-term release of DHP and its antimicrobial activity against *P. aeruginosa* and other detrimental biofilm-forming bacteria. This composite is proposed to be healing agent suitable for application in a form of dressing with prolonged effect on wounds.

2. Materials and Methods

2.1. Synthesis of BC, DHP, and preparation of the BC-DHP composite hydrogel

The bacteria culture *Komagataeibacter intermedius* IMBG180 (the collection of microorganisms of the Institute of Molecular Biology and Genetics, Kyiv, Ukraine) was used for the cellulose-based pellicle production. The culture was grown in HS medium [38] for 5

days at 30 °C. After incubation, the bacterial cellulose synthesized on the surface of the medium was harvested and purified with the method described in details by Kukharenko et al. [20].

The DHP of coniferyl alcohol (CA; Sigma Aldrich, Germany) was synthesized according to the procedure described in detail in [35]. Briefly, the reaction mixture of CA, H_2O_2, and horseradish peroxidase (Sigma Aldrich, Germany) was prepared in phosphate buffer, pH 7.3. After mixing and shaking the resulting suspension of DHP was centrifuged and washed in doubly distilled water. Finally, the precipitate was air-dried and dissolved in 5% dimethyl sulfoxide (DMSO) water solution.

It was shown that BC pellicles pre-treated with 100% DMSO better bound DHP (*see the Results section 3.3*). In all here reported analyses, sterile purified BC membranes were used, pre-soaked in 100% DMSO for 24 h and then in different DHP solutions (0.5, 1 and 5 mg/mL; BC-$DHP_{0.5}$, BC-$DHP_{1,}$ and BC-DHP_5, respectively) for 48 h. The BC hydrogels treated only with 100% DMSO were used as the control.

2.2. Fourier Transform Infrared (FT-IR) absorption spectroscopy

To assess the structural differences in BC-$DHP_{0.5}$ and BC-DHP_5 composite hydrogels in comparison with control BC the vibrational modes spectroscopy was used. Each sample was air dried on a glass slide in the form of a thin film. The film thickness was 0.025 - 0.03 mm. The IR absorption analysis was carried out with a Bruker-113v Fourier transform IR spectrometer. The measurements were performed at room temperature in the range of 500 – 4000 cm^{-1} with a spectral resolution of 1.0 cm^{-1}.

2.3. Scanning Electron Microscopy (SEM) and Atomic Force Microscopy (AFM) imaging

The control BC and BC-$DHP_{0.5}$, BC-DHP_1 and BC-DHP_5 composite samples (untreated and treated with 100% DMSO prior DHP impregnation) were coated with gold and studied using a ZEISS EVO 50XVP scanning electron microscope, equipped with INCA450 X-ray energy

spectrum analyzer with INCAPentAFETx3 detector and HKL CHANNEL-5 system for diffraction of reflected electrons produced by Oxford Instruments (Witney, United Kingdom). Detailed information on the surface topography of all samples was obtained using the Atomic Force Microscope (NT-MDT Ntegra SPM) in Semicontact Error Mode. The scanning frequency was kept at 0.74 Hz, meaning that the step size in the recorded images of 50×50 and 100×100 nm was 0.20 and 0.39 nm, respectively. The cantilever oscillation amplitude (i.e. Set Point) during the measurements was 6.0 V. The recorded images in Height represent the surface topography, while the images Mag (Magnitude) represent so-called error signal which provides higher contrast for sharp features on the surface. The chosen scanning mode enables BC filaments to be more distinct from DHP globules in the recorded images, and moreover, it enables precise determination of shape and dimensions of all surface features.

2.4. X-Ray Diffraction (XRD)

The phase composition of control BC, BC-$DHP_{0.5}$, BC-DHP_1 and BC-DHP_5 composite samples was examined by X-ray diffraction (Raguku Ultima IV, Japan). The X-ray beam was nickel-filtered CuKα1 radiation (λ = 0.1540 nm, operating at 40 kV and 40 mA). XRD data were collected from 3° to 45° (2θ) at a scanning rate of 2°/min. Phase analysis was done by using the PDXL2 software (version 2.0.3.0, 2011, Rigaku Corporation, Tokyo, Japan) with reference to the patterns of the International Centre for Diffraction Data database version 2012. The crystallinity (X_c) of all samples was calculated from the relative integrated area of the crystalline and amorphous peaks by applying the equation: $X_c=(A_{cr}/(A_{cr}+A_{am}))$x100, where A_{cr} and A_{am} were the integrated areas of the crystalline and amorphous peaks after deconvolution of experimental patterns [39].

2.5. Water holding capacity (swelling degree) of the composite hydrogel

The control BC, BC-$DHP_{0.5}$, BC-DHP_1 and BC-DHP_5 composite samples were cut into pieces 3×2×0.3 cm large and lyophilized for 24 h. All samples were weighted and then

soaked in deionized water for 72 h. The water holding capacity or swelling degree presented in percentage was calculated as follows: Swelling degree(%)=((W_s-W_i)/W_i)x100, where *Wi* was the initial weight of the dried sample and *Ws* was the weight of sample after soaking in water. The swelling degree was calculated at time intervals: 15th, 30th, 45th, 60th min, 2nd, 3rd, 24th, 48th and 72th h. All experiments were performed in triplicate. Kruskal-Wallis H test followed by post hoc Dunn's test was used to evaluate the differences between control and composite samples.

2.6. Antibacterial activity of BC-DHP composite hydrogel

The following Gram-negative *P. aeruginosa* (ATCC 27853) and *S. typhimurium* (ATCC 13311) and Gram-positive bacteria *L. monocytogenes* (NCTC 7973) and *S. aureus* (ATCC 6538) were used. The organisms were obtained from Mycological Laboratory, Department of Plant Physiology, Institute for Biological Research "Siniša Stanković", University of Belgrade, Serbia. The other bacterial isolates (*S. aureus* #1*; *S. aureus* #2*, *P. aeruginosa**; and *Serratia* sp.*) were human isolates obtained from patients at the Department of Microbiology, Clinical Center of Serbia, Belgrade, Serbia. Bacteria were cultured on Muiller Hinton Agar (MHA, Merck, Germany) at 37 ˚C for 24 h. The antibacterial test of BC-DHP membranes was carried out by modified microdilution method [40] in bacterial suspensions with sterile saline to a concentration of 1.0 x 10^5 CFU/mL measured on densitometer DEN-1B (Biosan, Latvia). The minimum inhibitory and bactericidal concentrations (MICs and MBCs) were determined using 96-well microtitre plates. The BC-DHP membranes 7 mm in diameter were added in Triptic Soy broth (100 μL) with the bacterial inoculum (1.0 x 10^5 CFU per well). The concentrations in wells of released DHP from BC-DHP discs, BC-DHP$_1$, BC-DHP$_{2.5}$, and BC-DHP$_5$, were determined by measuring absorbance at 272 nm after 24 hours and were 0.22, 0.42 and 0.88 mg/mL, respectively. The microplates were incubated at rotary shaker (160 rpm) for 24 h at 37 °C. The lowest concentrations without visible growth

(at the binocular microscope) were defined as concentrations that completely inhibited bacterial growth (MICs). The MBCs were determined by serial sub-cultivation of 5 µL into microtiter plates containing 100 µL of broth per well and further incubation for 24 h. The lowest concentration with no visible growth was defined as MBC, indicating 99.5% killing of the original inoculum. All experiments were performed in triplicate.

2.7. In vitro *release of DHP from the BC-DHP composite hydrogel*

The control BC and BC-DHP_1 composite membranes were cut into disks 28 mm in diameter and 1 mm average thickness. *In vitro* release of DHP from the composite samples was monitored in 15 mL PBS, pH 7.4. All experiments were performed at 37 ºC with constant shaking at 100 rpm. Aliquots of the sample (1 mL) were taken at predetermined time intervals (1, 2, 3, 24, 48 and 72 h) and concentration of DHP in dissolution media was determined spectrophotometrically (Shimadzu, Kyoto, Japan) at 272 nm. Immediately after measuring absorbance, aliquots were poured back into dissolution media, to maintain a constant volume. All experiments were performed in duplicate.

2.8. High-Performance Liquid Chromatography and Mass Spectrometry (HPLC/MS) analysis

Reversed phase HPLC/MS analysis was used for qualitative analysis of dissolved DHP samples: bulk DHP solution, released DHP fragments from BC-DHP_5 (released DHP fraction) and non-adsorbed DHP after removing BC-DHP_5 from DHP solution (unbound DHP fraction). The analyzed samples were dissolved in methanol and filtered through 0.22 µm pore-size filters. The samples were injected in Waters HPLC system consisted of 1525 binary pumps, thermostat and 717+ auto sampler connected to the Waters 2996 diode array and EMD 1000 Single quadrupole detector with ESI probe (Waters, Milford, USA). Separation was performed on a Symmetry C-18 RP column 125x4 mm size packed with 5 µm diameter particles (Waters, Milford, MA, USA) connected to appropriate guard column.

Two mobile phases, A (0.1% formic acid) and B (acetonitrile) were used at flow of 1 mL min^{-1} with the following gradient profile: the first 20 min from 10 to 20% B; next 10 min of linear rise up to 40% B, from 30 to 45 min 70% B is reached followed by 5 min reverse to initial 10% B and additional 5 min for column equilibration. Post column flow splitter (ASI, Richmond, CA, USA) with 5/1 split ratio was used to obtain optimal mobile phase inflow for ESI probe. UV signals were recorded in DAD scan mode from 200-650 nm and specific chromatograms were extracted at 271 nm. For LC/MS analysis, signals for each compound were recorded in negative scan mode with following parameters: capillary voltage 3.0 kV, cone voltage -35 V, extractor and RF lens voltages were 3.0 and 0.2 V respectively. Source and desolvation temperatures were 120 ^{o}C and 380 ^{o}C, respectively, with N_2 gas flow of 550 L\h. The data acquisition and spectral evaluation for peak confirmation were carried out by the Waters Empower 2 Software (Waters, Milford, USA).

3. Results and discussion

3.1. Synthesis of bacterial cellulose-lignin composite hydrogel

As hydrogels, natural polymers and composite materials, represent both a bandage and a matrix for therapeutics in wound healing, the new composite hydrogel based on bacterial cellulose and lignin model polymer was designed. *K. intermedius* synthesizes the pure form of BC, which does not require intensive processing to remove bacterial cell and metabolites. Sterile purified BC membranes, pre-soaked in 100% DMSO for 24 h and then in different DHP solutions (0.5, 1 and 5 mg/mL; BC-$DHP_{0.5}$, BC-DHP_1 and BC-DHP_5, respectively) for 48 h, were characterized and used in antibacterial analysis (Fig. 1).

3.2. FT-IR absorption spectroscopy

The absorption spectra for DHP, control BC, BC-$DHP_{0.5}$ and BC-DHP_5 membranes are shown in Fig. 2. The BC-$DHP_{0.5}$ absorption spectrum was insignificant in comparison with control BC. Noticeable changes were observed in the spectrum with BC-DHP5. The decrease

of the bands characteristic for DHP in the spectrum of BC-DHP on one side and increase of certain bands characteristic for BC on the other is an indicator of interaction between DHP and BC. Namely, the DHP bands at: 824 and 861 cm^{-1} (C-H out-of-plane vibration in positions 2, 5, 6 in G units), 970 cm^{-1} (HC=CH out of plane deformation (trans)), 1035 cm-1 (aromatic C-H in plane deformation), 1141 cm^{-1} (aromatic C-H in plane deformation), 1220 cm^{-1} (C-C plus C-O plus C=O stretch, G condensed>G etherified), 1272 cm^{-1} (G ring plus C=O stretch), 1420 cm^{-1} (aromatic skeletal vibration combined with C-H in plane deformation), 1462 cm^{-1} (C-H deformations; asymmetric in CH3 and CH2) and 1512 cm^{-1} (aromatic skeletal vibrations) [41, 42] were decreased in the spectrum of BC-DHP. The bands at 1602 cm^{-1} (C=C aromatic) and 1660 cm^{-1} (C=C in side chain) in BC-DHP were slightly shifted in different directions: 1602 to 1599, and 1660 to 1667. This can testify that the vibrations were disturbed by the environment. On the other side, there was an increase in the cellulose bands at 1111, 1126 cm^{-1} (C-O, C-C from C-2-O-2) and at 1162 cm^{-1} (C-O-C glycoside link, ring) characteristic for BC, while the bands at 1281, 1315 cm^{-1} (CH2 wagging), 1336, 1362 cm^{-1} (O-H in plane bending), 1372 and 1428 cm^{-1} (CH2 scissoring) [43] are not changed considerably. Decrease of the characteristic lignin bands indicates changing DHP environments during complexation with cellulose, which is an indicator of binding.

The typical BC bonds were observed in composite spectra, e.g., β-1,4 glycosidic bonds absorption band at 897 cm^{-1}[44]. When considering the BC-DHP_5 spectra in comparison to control BC, although a weak interaction, an appearance of a new band at 3293 cm^{-1} could serve as a proof of the impregnation of DHP in BC. Deformed S=O sulfoxide group vibrations (attributed to DMSO, used as DHP solvent) had been revealed in BC-DHP composite samples in 1070 – 1030 cm^{-1} spectral range. DMSO as the electron accepter [45] could cause the peak shifts to lower wavenumbers. At the same time, while intensity of

absorption bands related to BC were enhanced somewhere in BC-DHP up to 3 times, e.g., at 1111-1126 cm^{-1} and at 1162 cm^{-1}, a vibration mode of the C(1)-H(β)/COC was practically undisturbed. This may indicate that cellulose molecules are in different orientations in the presence of DHP, comparing to ones of its absence.

The increase of certain cellulose bands indicates that cellulose molecules are in different orientations in the presence of DHP, comparing to the orientations in its absence, which is an indication of binding. Based on the absorption spectra, the IR crystallinity index (abs. at 1427/895 cm^{-1}) [46] calculated for all samples showed a dose-dependent increasing of crystallinity for BC-DHP composites. The values of IR crystallinity index were 3.4, 4.0 and 4.25 for control BC, BC-$DHP_{0.5}$ and BC-DHP_5, respectively. Obviously, the changes in BC-$DHP_{0.5}$ occurred but they were not observed in absorption spectrum due to the low sensitivity of absorption spectroscopy.

3.3. SEM and AFM imaging

In Fig. 3, SEM images of control BC and BC-DHP composite samples (BC-$DHP_{0.5}$, BC-DHP_1, BC-DHP_5) untreated and treated with 100% DMSO before impregnation with DHP are shown.

It was found a dose-dependent decrease in the amount of pores in the composite samples treated with DMSO. BC-DHP_5 was almost completely lacked in pores. The average pore sizes were 123.6 nm for BC-$DHP_{0.5}$ and 52.7 nm for BC-DHP_5. This effect was not observed in the BC-DHP samples not treated with DMSO. Therefore, it can be assumed that the treatment of BC membranes with DMSO significantly increased the ability of DHP to bind to BC filaments/fibers.

In cellulose polymer, glucose chains are forming fibers, which are further aggregating in ribbons (3 nm), and these ribbons, aggregating in filaments (30-100 nm), subsequently form a web-shaped network structure [47]. The control BC sample in this study showed nanoscale

network structure with filaments of size <30 nm, which are smaller than previous published [20, 48].

The topography of control BC and BC-DHP composite samples is presented in Fig. 4. The control BC sample consisting of the interconnected network of BC fibers organized into filaments 20 nm in diameter, was porous and with the noticeable smooth texture of background areas. All BC-DHP samples exhibited rough multiphase structure, consisting of a continuous network of BC fibers/filaments, randomly organized pores and DHP globules. The branching interconnected fibers were fairly uniform in width, which was in the range of 0.7 - 2.7 nm. On the other side, the synthetic analogue of lignin, DHP, is a branched molecule with the tendency to form globules organized in an onion like layered structure [49, 50]. In BC-DHP samples, depending on the concentration of DHP, AFM topography images showed randomly spread or attached to the surface elongated or irregular spherical particles, mostly oligomers of low and moderate molecular weights. In BC-$DHP_{0.5}$ and BC-DHP_1 composite samples the size of DHP globules was predominantly in the range of 4 – 8 nm. In BC-DHP_5 hydrogel DHP globules were more visible with a tendency to form larger irregular architectures in the range of 4 – 12 nm. The size of the globules is mostly in agreement with structures previously identified by AFM [51].

3.4. *XRD characterization and water holding capacity (swelling degree) of the composite hydrogel*

The XRD patterns of the control BC, BC-$DHP_{0.5}$, BC-DHP_1 and BC-DHP_5 composite samples are presented in Fig. 5. All the samples were amorphous but showed peaks at 2θ at 14.2°, 16.7°, and 22.7°, corresponding to the (1-10), (200) and (110) Miller indices of microbial cellulose [52]. The lowest intensity of peaks was noticed for the control BC and with increasing of the concentration of DHP the intensity of peaks also increased (BC-$DHP_{0.5}$ < BC-DHP_1 < BC-DHP_5). The values of full width at half maximum (FWHM) for control

BC, BC-$DHP_{0.5}$, BC-DHP_1 and BC-DHP_5 composite samples were 81.97, 9.68, 9.85, 9.64, respectively. The degree of crystallinity (X_c, in percentage) for control BC, BC-$DHP_{0.5}$, BC-DHP_1 and BC-DHP_5 composite samples were 62.07, 70.22, 72.26, 74.38, respectively. The obtained results of crystallinity degree confirmed diffractograms of the samples presented in Fig. 5, clearly indicating dose-dependent crystallinity for BC-DHP composite samples. Crystallinity, as a demonstration of hydrophobicity of the material [53] and swelling, as a demonstration of hydrophilicity, are in close relation. Swelling ability or the ability of water to penetrate into the structure [54] is very important dressings' characteristic [55]. The results of water holding capacity (swelling ability) during 72 h are shown in Fig. 6.

In the first 15 min of dipping in water, all the samples reached more than 3 times of their initial weight. During the monitoring time the swelling degree increased and showed dose-dependent behavior (control > BC-$DHP_{0.5}$ > BC-DHP_1 > BC-DHP_5). The control BC had the highest holding capacity in the range of 86 – 97%. The composite samples had a swelling degree in the range of 83 – 97%, 78 – 93% and 74 – 88% for BC-$DHP_{0.5}$, BC-DHP_1, and BC-DHP_5, respectively. Kruskall-Wallis and Dunn's post hoc test showed significant differences in water holding capacity between the samples after 48 h ($H_{(4,12)48\ h} = 9.462$ and $H_{(4,12)72\ h} = 10.380$, $p<0.5$; where $H_{(number\ of\ groups,\ number\ of\ values)}$ - Kruskal-Wallis chi-squared value). Obtained results showed that BC-$DHP_{0.5}$ composite had the best ability to absorb water during the whole monitoring time. The crystalline region of cellulose does not allow water to enter its region as it caused lower swelling ability of the material [56]. That theory was proven by the preceding study [57] showing that the lower the crystallinity of cellulose powder, the higher was the moisture sorption. Herein, control BC was the most amorphous sample and with the best ability to absorb water (97%) with the crystallinity index of 62%, which is similar to previously reported studies [58, 59]. Swelling capacities of the BC-DHP composites were predicted from the calculated degree of crystallinity. The crystallinity of

composites increased and their swelling ability decreased in a dose-dependent manner. Also, the IR crystallinity index revealed an increase in crystallinity for BC-$DHP_{0.5}$ in 1.26 and for BC-DHP_5 in 1.43 times. All mentioned characteristics are in coexistence with previously reported results where control BC had lower crystallinity than composites with pectin and xyloglucan [60].

3.5. *Antibacterial activity of BC-DHP composite hydrogel*

The antibacterial activity of BC-DHP membranes is shown in Table 1. BC-DHP exhibited antibacterial activity on all tested bacteria, with exception of *P. aeruginosa* and *S. aureus* #1*. The inhibition potential was only obtained towards *S. aureus* #2* and *S. typhimurium*, while the bactericidal effect was not achieved. Minimal inhibitory and bactericidal concentrations of DHP that were effective against *L. monocytogenes* and *Serratia* sp.* were in the range of 0.22-0.88 mg/mL. Bactericidal activity was observed against *P. aeruginosa** at all tested concentrations of DHP, while *S. aureus* was sensitive at MBC 0.88 mg/mL. Based on the obtained results, where BC-DHP hydrogel was effective against *P. aeruginosa*, *S. aureus,* and *Serratia* sp. isolated from the patients' chronic wounds, it has a potential to be used in

medical treatments as antibacterial dressing.

3.6. In vitro *release of DHP from the composite hydrogel*

Fig. 7A shows release profile of DHP from BC-DHP_1 membranes. It is obvious that after an initial burst release of 34% in the first hour, BC-DHP membranes allowed slow and continuous release of DHP in PBS solution. After 24 hours of faster release rate, BC continued to release small amounts of DHP for the next 72 hours. After 72 hours, released amount of DHP was 46.2%. The intensive release of DHP in the first hours could be beneficial for patients to prevent spreading an infection at the beginning of wound infection

therapy, while keeping the constant higher concentration of antimicrobial compound for the next 72 h is suitable for maintaining antimicrobial capacity.

In order to characterize the mechanism of DHP release, the experimental data were fitted into different mathematical models, such as: zero-order, first-order, Higuchi and Korsmeyer-Peppas kinetic model. The highest value of correlation coefficient (R^2) was obtained for the Korsmeyer-Peppas model (with the equation: $Mt/M\infty=ktn$, where n is the release exponent related to the mechanism of the release). The n value was smaller than 0.5 (Fig. 7B) indicating that the release of DHP from BC-DHP composite can be characterized as a quasi-Fickian diffusion [61, 62]. All obtained results of *in vitro* DHP release study also showed that it was partially governed by DHP diffusion throughout the BC polymeric mesh and was dependent on the high swellability of the BC membranes. Lower water solubility of larger oligomers of DHP and their possible electrostatic interactions with BC could be responsible for the 50% of unreleased DHP from the membranes.

3.7. HPLC/MS analysis

Fig. 8 represents chromatograms recorded at 271 nm, for DHP solution, released DHP fraction and unbound DHP fraction. All chromatograms show qualitatively similar peaks but with significant quantitative differences in regions characteristic for different size of CA oligomers.

Peak 1 is characterized by the main signal of 327 m/z followed by 195 and 179 m/z fragments and low intensity signal of 375 m/z which could be attributed to the 8-O-4 dimer. Peak 2 shows the similar fragmentation pattern but with the major signal at 195 m/z and lower at 327 and 179 m/z may originate from 8-O-8. The most prominent peak (3) recorded at 271 nm has two major MS signals at 339 and 327 m/z, respectively, with low-intensity signal recorded at 357 m/z, corresponding to the 8-5 dimer (Fig. 8.S1). Peaks 4 and 5 are characterized by the main signal at 327 m/z followed by 179 and 389 m/z which could

originate from 8-8 linked dimer moiety. Peaks 6 and 7 have the strongest signal at 357 m/z followed by 179 m/z and the weak signal at 537 m/z suggesting trimer structure with 8-8 linking pattern (Fig. 8.S2).

In general, most of the DHP peaks gave the signals characteristic for CA dimers, trimers and tetramers (327 m/z; 339 m/z; 357 m/z; 535 m/z and 713 m/z) [63]. Since the single quadrupole is used, a detailed structural analysis is unreliable but the positive correlation of expected longer retention times with CA oligomers size argue in favor of such peak evaluation. The HPLC/MS analysis showed that larger oligomers are more abundant in DHP solution in comparison with the released DHP fraction and unbound DHP fraction. This indicates that BC binds larger oligomers and releases smaller oligomers. These results are in accordance with the results of *in vitro* release of DHP from BC-DHP composite membranes. Comparing with the literary data, the most probable types of bonds in the DHP oligomers are 8-O-4, 8-8 and 8-5, which are typical for this lignin model polymer [64]. The released compounds, mostly dimers and trimers, may be antimicrobially active DHP fractions.

4. Conclusion

The novel synthesized composite based on bacteria cellulose and lignin model polymer, BC-DHP, designed in the form of dressing, showed an inhibitory/bactericidal effect against clinically isolated biofilm-forming bacteria *P. aeruginosa, S. aureus* and *Serratia* sp. and laboratory strains ones *S. aureus, L. monocytogenes,* and *S. typhimurium. In vitro* release analysis showed the intensive release of DHP in the 1st h and keeping the constant higher concentration of antimicrobial compounds for the next 72 h. HPLC/MS analysis confirmed that released compounds were mostly dimers and trimers of CA. Since BC-DHP composite showed high swellability and prolonged release of antibacterial compounds, which could be beneficial for patients to firstly prevent spreading an infection and then to maintain

antimicrobial capacity, it is suitable for pre-clinical trials as a promising agent for chronic wounds healing.

5. Acknowledgements

This study was financially supported by the Ministry of Education, Science and Technological Development of the Republic of Serbia [grants III45012, 173017, III45007, 173040, 173032] and the National Academy of Sciences of Ukraine (grant 47/2015-2016). Thanks to Khirunenko Ludmila from Institute of Physics, Kyiv, Ukraine, for professional assistance in clarification of absorbance bands.

6. Disclosures

Conflict of interest: The authors declare no competing financial interest.

7. References

[1] D. Klemm, D. Schumann, F. Kramer, N. Heßler, M. Hornung, H.P. Schmauder, S. Marsch, Nanocelluloses as innovative polymers in research and application, Polysaccharides II. 205 (2006) 49–96.

[2] S.M. Keshk, Bacterial cellulose production and its industrial applications, J. Bioprocess. Biotech. 4 (2014) 150.

[3] G. Helenius, H. Bäckdahl, A. Bodin, U. Nannmark, P. Gatenholm, B. Risberg, In vivo biocompatibility of bacterial cellulose, J Biomed Mater Res A. 76(2) (2006) 431-438.

[4] R.A. Pértile, S. Moreira, R.M. Gil da Costa, A. Correia, L. Guãrdao, F. Gartner, M. Vilanova, M. Gama, Bacterial cellulose: long-term biocompatibility studies, J Biomater Sci Polym Ed. 23(10) (2012) 1339-1354.

[5] F.K. Andrade, J.P. Silva, M. Carvalho, E.M. Castanheira, R. Soares, M. Gama, Studies on the hemocompatibility of bacterial cellulose, J Biomed Mater Res A. 98(4) (2011) 554-566.

[6] J. Andersson, H. Stenhamre, H. Bäckdahl, P. Gatenholm, Behavior of human

chondrocytes in engineered porous bacterial cellulose scaffolds, J Biomed Mater Res A. 94(4) (2010) 1124-1132.

[7] Q. Shi, Y. Li, J. Sun, H. Zhang, L. Chen, B. Chen, H. Yang, Z. Wang, The osteogenesis of bacterial cellulose scaffold loaded with bone morphogenetic protein-2, Biomaterials. 28(33) 6644-6649.

[8] C. Brackmann, M. Zaborowska, J. Sundberg, P. Gatenholm, A. Enejder. In situ Imaging of Collagen Synthesis by Osteoprogenitor Cells in Microporous Bacterial Cellulose Scaffolds, Tissue Eng Part C Methods. 18(3) (2012) 227-234.

[9] D.R. Solway, M. Consalter, D.J. Levinson, Microbial cellulose wound dressing in the treatment of skin tears in the frail elderly, Wounds – A Compendium of Clinical Research and Practice. 22(1) (2010) 17-19.

[10] P. Muangman, S. Opasanon, S. Suwanchot, O. Thangthed, Efficiency of Microbial Cellulose Dressing in Partial-Thickness Burn Wounds, J Am Col Certif Wound Spec. 3(1) (2011) 16-19.

[11] A.B. Moniri, S. Moghaddam, R.A. Azizi, A.B. Rahim, W.Z. Ariff, M. Saad, Navaderi, R. Mohamad, Production and Status of Bacterial Cellulose in Biomedical Engineering, Nanomaterials. 7 (2017) 257.

[12] L. Fu, Y. Zhang, C. Li, Z. Wu, Q. Zhuo, X. Huang, G. Qiu, P. Zhou, G. Yang, Skin tissue repair materials from bacterial cellulose by a multilayer fermentation method, J. Mater. Chem. 22 (2012) 12349-12357.

[13] L. Fu, P. Zhou, S. Zhang, G. Yang, Evaluation of bacterial nanocellulose-based uniform wound dressing for large area skin transplantation, Mater Sci Eng C Mater Biol Appl. 33(5) (2013) 2995-3000.

[14] B. Wei, G. Yang, F. Hong, Preparation and evaluation of a kind of bacterial cellulose dry films with antibacterial properties, Carbohydr Polym. 84(1) (2011) 533-538.

[15] K. Ghule, A.V. Ghule, B.J. Chen, Y.C. Ling, Preparation and characterization of ZnO nanoparticles coated paper and its antibacterial activity study, Green Chem. 8 (2006) 1034-1041.

[16] J.P. Ruparelia, A.K. Chatterjee, S.P. Duttagupta, S. Mukherji, Strain specificity in antimicrobial activity of silver and copper nanoparticles, Acta Biomater. 4(3) (2008) 707-716.

[17] Y. Zhang, H. Peng, W. Huang, Y. Zhou, D. Yan, Facile preparation and characterization of highly antimicrobial colloid Ag or Au nanoparticles, J. Colloid Interface Sci. 325(2) (2008) 371-376.

[18] J. Wu, Y. Zheng, W. Song, J. Luan, X. Wen, Z. Wu, X. Chen, Q. Wang, S. Guo, In situ synthesis of silver-nanoparticles/bacterial cellulose composites for slow-released antimicrobial wound dressing, Carbohydr Polym. 102 (2014) 762-771.

[19] S. Berndt, F. Wesarg, C. Wiegand, D. Kralisch, F. Muller, Antimicrobial porous hybrids consisting of bacterial nanocellulose and silver nanoparticles, Cellulose. 20 (2013) 771-783.

[20] O. Kukharenko, J.F. Bardeau, I. Zaets, L. Ovcharenko, O. Tarasyuk, S. Porhyn, I. Mischenko, A. Vovk, S. Rogalsky, N. Kozyrovska, Promising low cost antimicrobial composite material based on bacterial cellulose and polyhexamethylene guanidine hydrochloride, Eur. Polym. J. 60 (2014) 247–254.

[21] S. Napavichayanun, P. Amornsudthiwat, P. Pienpinijtham, P. Aramwit, Interaction and effectiveness of antimicrobials along with healing-promoting agents in a novel biocellulose wound dressing, Mater Sci Eng C Mater Biol Appl. 55 (2015) 95-104.

[22] S. Napavichayanun, R. Yamdech, P. Aramwit, The safety and efficacy of bacterial nanocellulose wound dressing incorporating sericin and polyhexamethylene biguanide: in vitro, in vivo and clinical studies, Arch Dermatol Res. 308(2) (2016) 123-132.

[23] J. Cai, S. Kimura, M. Wada, S. Kuga, Nanoporous Cellulose as Metal Nanoparticles Support, Biomacromolecules. 10(1) (2009) 87–94.

[24] H.S. Barud, A.M. de Araújo Júnior, S. Saska, L.B. Mestieri, J.A. Campos, R.M. de Freitas, N.U. Ferreira, A.P. Nascimento, F.G. Miguel, M.M. Vaz, E.A. Barizon, F. Marquele-Oliveira, A.M. Gaspar, S.J. Ribeiro, A.A. Berretta, Antimicrobial Brazilian Propolis (EPP-AF) Containing Biocellulose Membranes as Promising Biomaterial for Skin Wound Healing, Evid Based Complement Alternat Med. 2013 (2013) 703024.

[25] H.G. de Oliveira Barud, R.R. da Silva, H. da Silva Barud, A. Tercjak, J. Gutierrez J, W.R. Lustri ,O.B.J. de Oliveira, S.J. Ribeiro, A multipurpose natural and renewable polymer in medical applications: Bacterial cellulose, Carbohydr Polym. 153 (2016) 406-420.

[26] S. Arola, T. Tammelin, H. Setälä, A. Tullila, M.B. Linder, Immobilization–Stabilization of Proteins on Nanofibrillated Cellulose Derivatives and Their Bioactive Film Formation, Biomacromolecules 13(3) (2012) 594-603.

[27] L.M. Sampaio, J. Padrão, J. Faria, J.P. Silva, C.J. Silva, F. Dourado, A. Zille, Laccase immobilization on bacterial nanocellulose membranes: Antimicrobial, kinetic and stability properties, Carbohydr Polym. 145 (2016) 1-12.

[28] Y. Pötzinger, D. Kralisch, D. Fischer, Bacterial nanocellulose: the future of controlled drug delivery?, Ther. Deliv. 8(9) (2017) 753–761.

[29] H. Adlercreutz, Phytoestrogens: epidemiology and a possible role in cancer protection, Environ Health Perspect. 103 (1995) 103–112.

[30] R.A. Dixon, Phytoestrogens, Annu Rev Plant Biol. 55 (2004) 225–261.

[31] E. Slavikova, B. Kosikova, Inhibitory effect of lignin by-products of pulping on yeast growth, Folia Microbiol. 39(3) (1994) 241–243.

[32] J.L. Nelson, J.W. Alexander, L. Gianotti, C.L. Chalk, T. Pyles, Influence of dietary fiber on microbial growth in vitro and bacterial translocation after burn injury in mice, Nutrition. 10(1) (1994) 32-36.

[33] V.K. Thakur, M.K. Thakur, Recent advances in green hydrogels from lignin: a review, Int J Biol Macromol. 72 (2015) 834-847.

[34] S. Thakur, P.P. Govender, M.A. Mamo, S. Tamulevicius, Y.K. Mishra, V.K. Thakur, Progress in lignin hydrogels and nanocomposites for water purification: Future perspectives, Vacuum. 146 (2017) 342-355.

[35] D. Spasojević, D. Zmejkoski, J. Glamočlija, M. Nikolić, M. Soković, V. Milošević, I. Jarić, M. Stojanović, E. Marinković, T. Barisani-Asenbauer, R. Prodanović, M. Jovanović, K. Radotić, Lignin model compound in alginate hydrogel: a strong antimicrobial agent with high potential in wound treatment, Int J Antimicrob Agents. 6(48) (2016) 732–735.

[36] D. Davies, Understanding biofilm resistance to antibacterial agents, Nat Rev Drug Discov 2. (2003) 114–122.

[37] J.W. Costerton, Z. Lewandowski, D.E. Caldwell, D.R. Korber, H.M. Lappin-Scott, Microbial biofilms, Annu Rev Microbiol. 49 (1995) 711–745.

[38] S. Hestrin, M. Schramm, Synthesis of cellulose by Acetobacter xylinum. 2. Preparation of freeze-dried cells capable of polymerizing glucose to cellulose, Biochem. J. 58 (1954) 345-352.

[39] B. Focher, M.T. Palma, M. Canetti, G. Torri, C. Cosentino, G. Gastald, Structural differences between non-wood plant celluloses: Evidence from solid state NMR, vibrational spectroscopy and X-ray diffractometry, Ind Crops Prod. 13 (2001) 193–208.

[40] M. Soković, J. Glamočlija, D.P. Marin, D. Brkić, L.V.G. van Griensven, Antibacterial Effects of the Essential Oils of Commonly Consumed Medicinal Herbs Using an In Vitro Model, Molecules. 15 (2010) 7532-7546.

[41] O. Faix, Investigations on lignin polymer modeis (DHP's) by FTIR Spectroscopy, Holzforschung. 40 (1986) 273-280.

[42] O. Faix, Fourier Transform Infrared Spectroscopy in Solid State. In: Dence, C. and S. Linn (Eds.): Methods in Lignin Chemistry. Springer-Verlag, Berlin, New York, 1991 in press

[43] M. Katchurakova, P. Capek, V. Sasinkova, N. Wellner, A. Ebringerova, FT-IR study of plant cell wall model compounds: pectic polysaccharides and hemicelluloses, Carbohydrate Polymers. 43 (2000) 195-203.

[44] H.G. Shirk, G.A. Greathouse, Infrared Spectra of Bacterial Cellulose, Anal. Chem. 24(11) (1952) 1774–1775.

[45] Y. Zhao, X. Liu, J. Wang, S. Zhang, Insight into the cosolvent effect of cellulose dissolution in imidazolium-based ionic liquid systems, J Phys Chem B. 117(30) (2013) 9042-9049.

[46] W. Czaja, D. Romanovicz, R. Malcolm Brown, Structural investigations of microbial cellulose produced in stationary and agitated culture, Cellulose. 11(3-4) (2004) 403-411.

[47] S.P. Lin, I.L. Calvar, J.M. Catchmark, J.R. Liu, A. Demirci, K.C. Cheng, Biosynthesis, production and applications of bacterial cellulose, Cellulose. 20(5) (2013) 2191-2219.

[48] E.E. Kiziltas, A. Kiziltas, D.J. Gardner, Synthesis of bacterial cellulose using hot water extracted wood sugars, Carbohydr Polym. 124 (2015) 131-138.

[49] M. Micic, I. Benitez, M. Ruano, M. Mavers, M. Jeremic, K. Radotic, V. Moy, R.M. Leblanc, Probing the lignin nanomechanical properties and lignin-lignin interactions using the atomic force microscopy, Chem. Phys. Lett. 347 (2001) 41–45.

[50] M. Micic, K. Radotic, M. Jeremic, D. Djikanovic, S.B. Kämmera, Study of the lignin model compound supramolecular structure by combination of near-field scanning optical microscopy and atomic force microscopy, Colloids Surf B Biointerfaces. 34 (2004) 33–40.

[51] S.M. Shevchenko, G.W. Bailey, Nanoscale morphology of lignins and their chemical transformation products, Tappi. 79 (1996) 227-237.

[52] M.W. Ullah, M. Ul-Islam, S. Khan, Y. Kim, J.K. Park, Structural and physico-mechanical characterization of bio-celluloseproduced by a cell-free system, Carbohydr Polym. 136 (2016) 908-916.

[53] L. Segal, J.J. Creely, Jr.A.E. Martin, C.M. Conrad, An empirical method for estimating the degree of crystallinity of native cellulose using the X-ray diffractometer, Text. Res. J. 29(10) (1959) 786-794.

[54] I. Castellano, M. Gurruchaga, I. Goni, The influence of drying on the physical properties of some graft copolymers for drug delivery systems, Carbohydr Polym. 34(1-2) (1997) 83-89.

[55] W. Czaja, A. Krystynowicz, S. Bielecki, R.M. Brown, Microbial cellulose - the natural power to heal wounds, Biomaterials. 27(2) (2006) 145-151.

[56] X. Jie, Y. Cao, J.J. Qin, J. Liu, Q. Yuan, Influence of drying method on morphology and properties of asymmetric cellulose hollow fibre membrane, J Membr Sci. 246(2) (2005) 157-165.

[57] A. Mihranyan, A.P. Llagostera, R. Karmhag, M. Stromme, R. Ek, Moisture sorption by cellulose powders of varying crystallinity, Int. J. Pharm 269(2) (2004) 433-442.

[58] S.P. Lin, Y.H. Huang, K.D. Hsu, Y.J. Lai, Y.K. Chen, K.C. Cheng, Isolation and identification of cellulose-producing strain Komagataeibacter intermedius from fermented fruit juice, Carbohydr Polym. 151 (2016) 827-833.

[59] M. Martínez-Sanz, R.T. Olsson, A. Lopez-Rubio, J.M. Lagaron, Development of electrospun EVOH fibres reinforced with bacterial cellulose nanowhiskers. Part I: Characterization and method optimization, Cellulose. 18(2) (2011) 335-347.

[60] A. Zykwinska, J.F. Thibault, M.C. Ralet, Competitive binding of pectin and xyloglucan with primary cell wall cellulose, Carbohydr Polym. 74 (2008) 957–961.

[61] G. Pritchard, Environmental testing of organic matrix composites, in: J. M. Hodgkinson (Editor), Mechanical Testing of Advanced Fibre Composites, Woodhead Publishing Series in Composites Science and Engineering, Elsevier, 2000, pp. 269-292.

[62] S. Sahoo, C. K. Chakraborti, P. K. Behera, Development and Evaluation of Gastroretentive Controlled Release Polymeric Suspensions Containing Ciprofloxacin and Carbopol Polymers, J. chem. 4(4) (2012) 2268-2284.

[63] K. Morreel, O. Dima, H. Kim, F. Lu, C. Niculaes, R. Vanholme, R. Dauwe, G. Goeminne, D. Inzé, E. Messens, J. Ralph, W. Boerjan, Mass Spectrometry-Based Sequencing of Lignin Oligomers, Plant Physiol. 153 (2010) 1464-1478.

[64] K. Radotic, S. Todorovic, J. Zakrzewska, M. Jeremic, Study of Photochemical Reactions of Coniferyl Alcohol. II. Comparative Structural Study of a Photochemical and Enzymatic Polymer of Coniferyl Alcohol, J. Photochem. Photobiol. 68 (1998) 703-709.

Figure captions

Fig. 1. Schematic presentation of the hydrogels preparation

Fig. 2 Fragments of the Fourier Transform Infrared absorption spectra (500-4000 cm^{-1}) for: control bacterial cellulose (BC), dehydrogenate polymer (DHP), BC-$DHP_{0.5}$ composite and BC-DHP_5 composite.

Fig. 3. Scanning electron microscopy images of: A - native BC; B - control BC (with 100% DMSO), C, E, G – BC-$DHP_{0.5}$, BC-DHP_1, BC-DHP_5 composite samples, respectively, untreated with 100% DMSO; D, F, H - BC-$DHP_{0.5}$, BC-DHP_1, BC-DHP_5 composite samples, respectively, treated with 100% DMSO. Scale bars 200 nm. In the insets in D and H pore sizes are denoted.

Fig. 4. Atomic force microscopy images (Height/Mag –Topography and Error signal, respectively) on the 100x100 nm and 50x50 nm sample area of all sample surfaces obtained by Semicontact Error Mode: A - control BC, B - BC-$DHP_{0.5}$ composite, C - BC-DHP_1 composite, D - BC-DHP_5 composite.

Fig. 5. X-ray diffractograms of control BC and BC-DHP composite samples (BC-$DHP_{0.5}$, BC-DHP_1 and BC-DHP_5)

Fig. 6. Water holding capacity (swelling degree) in percent of control BC and BC-$DHP_{0.5}$, BC-DHP_1 and BC-DHP_5 composite samples. *$p<0.5$; **$p<0.01$ (Kruskall-Wallis H test, Dunn's post hoc test)

Fig. 7. Release profile of DHP from BC-DHP composite hydrogel (A) and DHP release data fitted to Korsmeyer–Peppas kinetic model (B).

Fig. 8. Overlapped HPLC-UV chromatograms of DHP solution, released DHP fraction and unbound DHP fraction recorded at 271 nm. CA stands for monomeric coniferyl alcohol and peaks 1-12 represent dominant oligomers in analyzed solutions.

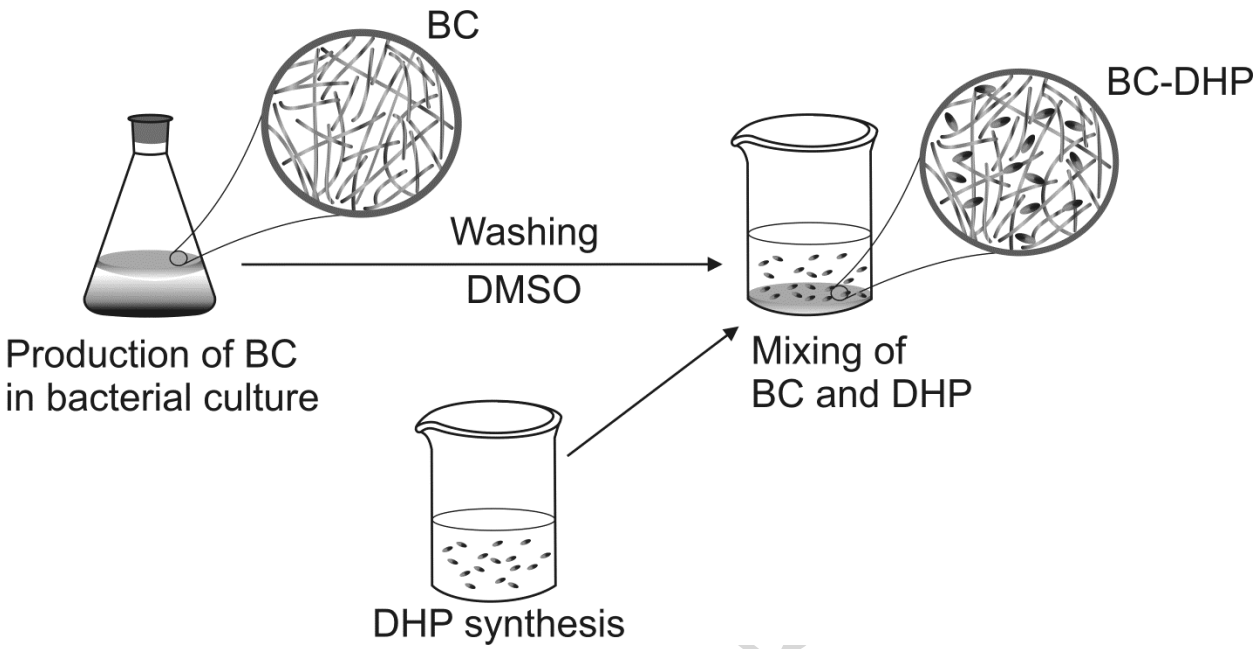

Fig. 1.

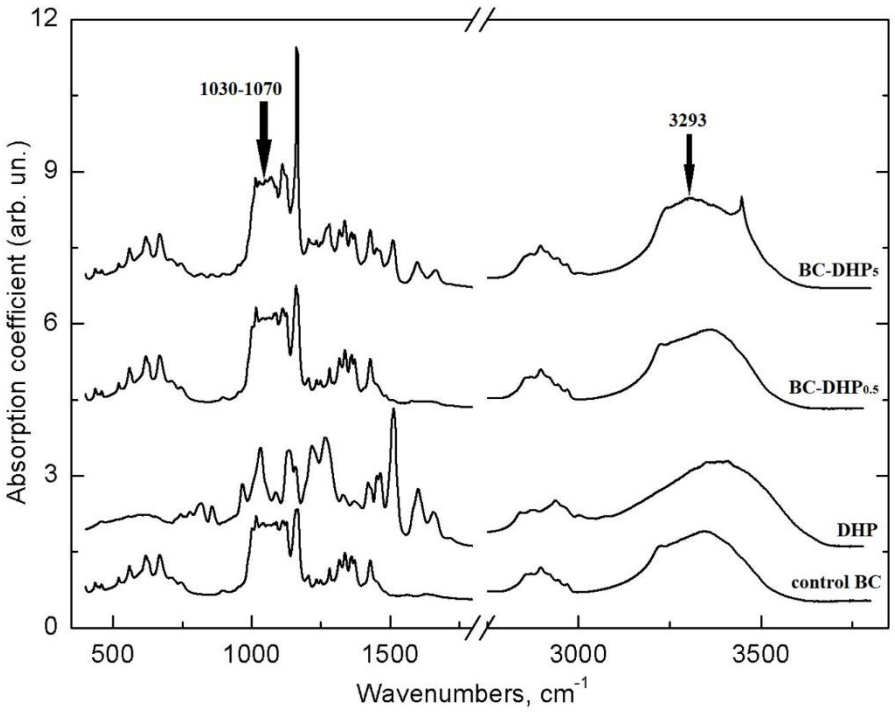

Fig. 2.

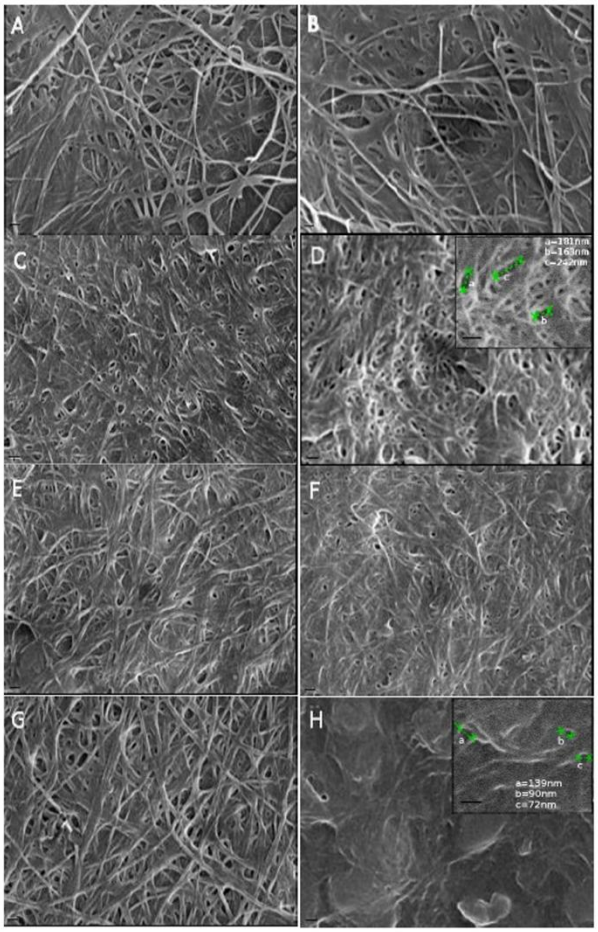

Fig. 3.

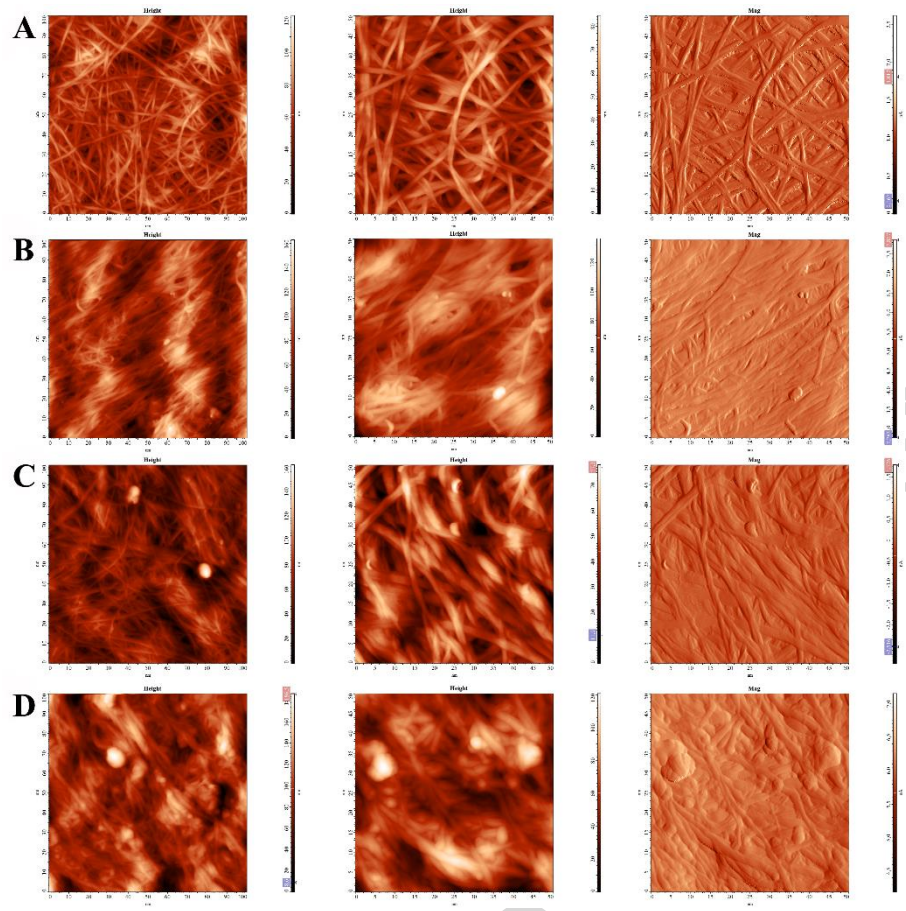

Fig. 4.

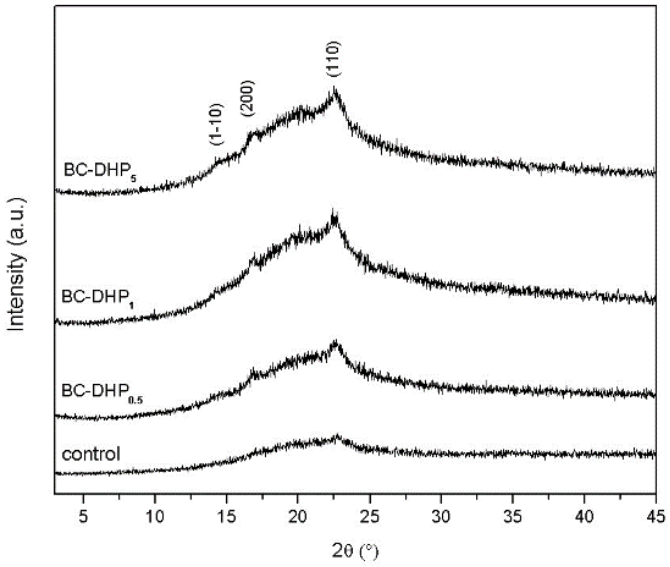

Fig. 5.

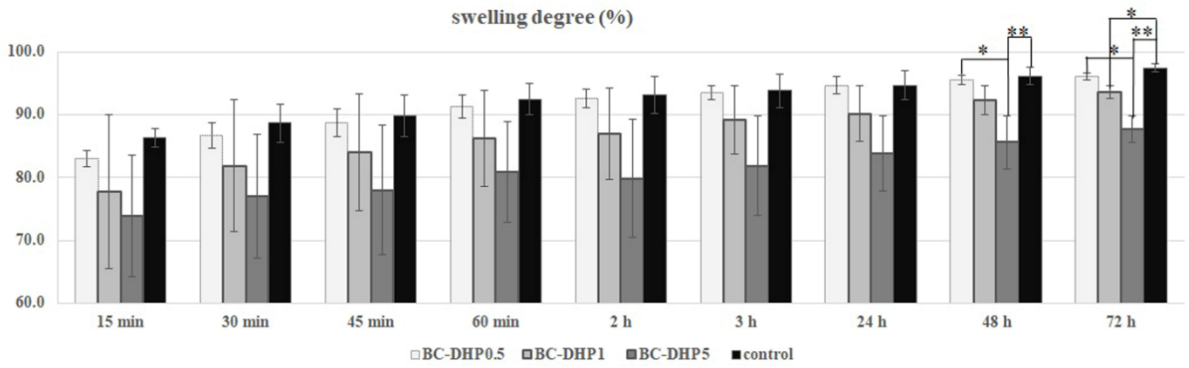

Fig. 6.

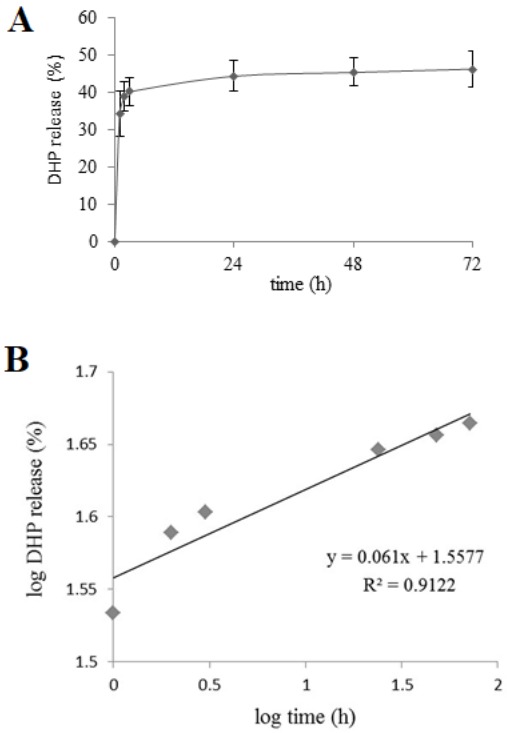

Fig. 7.

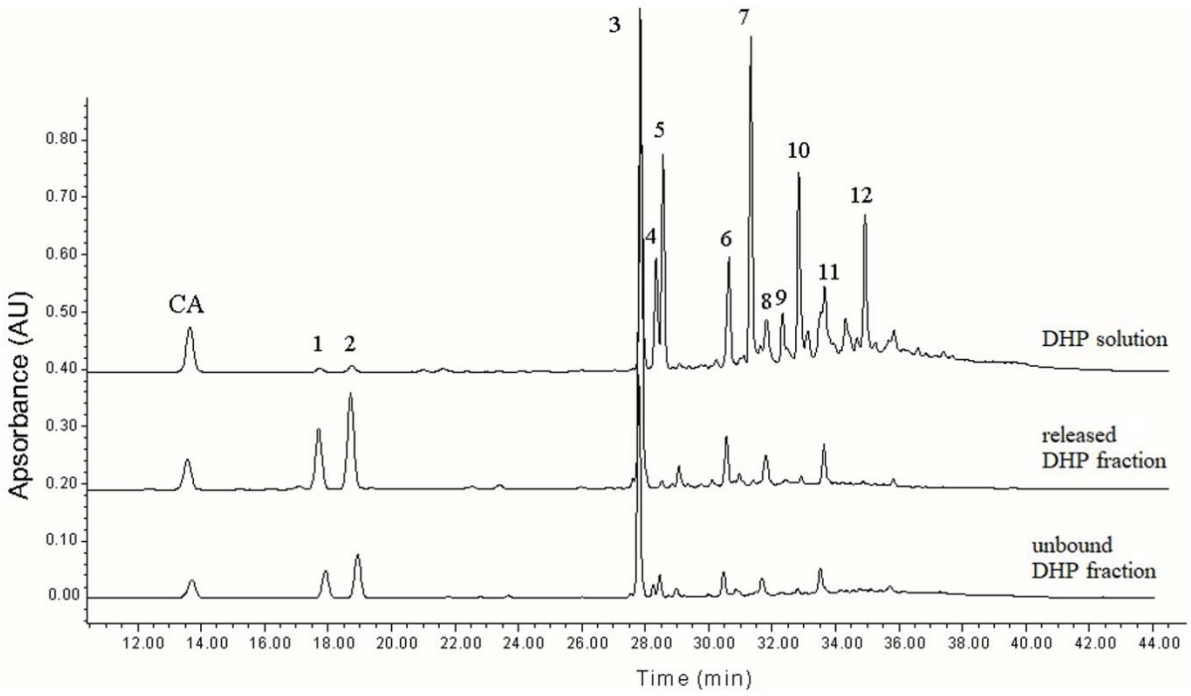

Fig. 8.

Table 1. Antibacterial activities of BC-DHP composite for the released DHP concentrations.

MIC - minimum inhibitory concentration; MBC - minimum bactericidal concentration

Bacteria	BC-DHP membranes (DHP concentrations in wells)		
	$BC\text{-}DHP_1$ (0.22 mg/mL)	$BC\text{-}DHP_{2.5}$ (0.42 mg/mL)	$BC\text{-}DHP_5$ (0.88 mg/mL)
	MIC/MBC	MIC/MBC	MIC/MBC
S. aureus (ATCC 6538)	-/-	-/-	-/+
S. aureus #1*	-/-	-/-	-/-
S. aureus #2*	+/-	-/-	+/-
L. monocytogenes (NCTC 7973)	+/-	+/-	-/+
P. aeruginosa (ATCC 27853)	-/-	-/-	-/-
*P. aeruginosa**	-/+	-/+	-/+
S. typhimurium (ATCC 13311)	-/-	+/-	+/-
Serratia sp.*	-/-	+/+	+/+

Highlights

- Novel composite BC-DHP in form of dressing showed inhibitory/bactericidal effect
- BC-DHP showed highest release of the active substance during the first 24 h
- Released active compounds were oligomers of coniferyl alcohol
- High swellability of hydrogel confirmed its potential role in chronic wound healing